International Journal of Minerals, Metallurgy and Materials
Volume 21, Number 7, July 2014, Page 682
DOI: 10.1007/s12613-014-0958-x

Observation of etch pits in Fe-36wt%Ni Invar alloy

Dong-zhu Lu and Min-jie Wu

Division of Surface Engineering of Materials, Institute of Metal Research, Chinese Academy of Sciences, Shenyang 110016, China

(Received: 28 November 2013; revised: 5 March 2014; accepted: 10 March 2014)

Abstract: To indirectly investigate the dislocation behavior of Fe–36wt%Ni Invar alloy by the etch pit method, polished Invar specimens were etched by a solution containing 4 g copper sulfate, 20 mL hydrochloric acid, and 20 mL deionized water for 2 min. Etch pits in the etched surfaces were observed. All the etch pits in one specific grain exhibited similar shapes, which are closely related to the grain orientations. These etch pits were characterized as dislocation etch pits. It was observed that etch pits arranged along grain boundaries, gathered at grain tips and strip-like etch pit clusters passed through a number of grains in the pure Invar specimens. After the addition of a small amount of alloying elements, the identification of a single dislocation etch pit is challenging compared with the pure Invar alloy. Thus, the observation of etch pits facilitates the investigation on the dislocation behavior of the pure Invar alloy. In addition, alloying elements may affect the densities and sizes of etch pits.

Keywords: Invar alloy; dislocations; etch pit technique; alloying elements

1. Introduction

After a considerable amount of etching, etch pits of various shapes and sizes emerge on the polished surfaces of metals. The optimal etching parameters are dependent on many factors [1], including the type of materials and the type and density of defects. The etching rates [2–3] and the morphology of etch pits [4–5] can be affected by the compositions of the etchants. Many etch pits are considered to be indications of the emergence of dislocations from the sample surface [6]. Evidence that etch pits are dislocation sites was obtained from deformation and annealing studies, and etch pit density counts on intersecting boundaries. Researchers have suggested that etch pits correspond to dislocations in crystals. One of the most convictive arguments is that the density of etch pits is closely related to the dislocation density [7–11]. Although numerous studies have demonstrated that etch pits are located at dislocations, the hypothesis that all dislocations are revealed by etch pits remains unproven [12].

Compared with previous methods that investigate the relationship between etch pits and dislocations using optical microscopes, a more precise investigation of GaN crystal was performed by researchers [13–14] using scanning electron microscopy (SEM), atomic force microscopy (AFM), focused ion beam (FIB), and transmission electron microscopy (TEM). Three types of distinctive etch pits (α-, β-, and γ-type etch pits) were observed on the etched GaN surfaces. By comparing the results of the SEM, AFM, and TEM, α-, β-, and γ-type etch pits were determined to correspond with screw, edge, and mixed-type thread dislocations, respectively.

Currently, dislocations in crystals are commonly investigated using TEM. TEM can be used to investigate heterogeneous microstructures and measure lower dislocation densities [15]; however, TEM provides insufficient data due to its limited field of view. Because the hypothesis that etch pits are sites where dislocations intersect with etched surfaces of samples has been experimentally proven, we can indirectly investigate dislocation behavior by observing etch pits on etched metal surfaces using an optical microscope or SEM. Although this method is not precise compared with traditional methods that employ TEM, it possesses specific advantages. For example, it enables the simple preparation and characterization of specimens. In addition, a larger field of view can be obtained. This method has been utilized to

Corresponding author: Dong-zhu Lu E-mail: dzlu11b@imr.ac.cn

investigate dislocations in many materials [16–18].

Fe–36wt%Ni Invar alloy is a single-phase alloy with an austenitic microstructure. Due to its low coefficient of thermal expansion (CTE), this alloy is extensively used in manufacturing parts, which are required to have high dimensional stability. To improve its performance, the effect of manufacturing processes on the microstructure of the Invar alloy should be investigated. Considering the feasibility of studying dislocation behavior by observing etch pits on crystal surfaces, which may increase the efficiency of studies, the dislocation etch pit technique was selected. In this paper, an optical microscope and SEM were employed to observe etch pits in Invar specimens. Using this method, dislocation behavior was investigated. The effect of alloying elements on etch pits in the Invar alloy was also explored.

2. Experimental

A pure Invar ingot was prepared from electrolytic iron and electrolytic nickel by vacuum melting and casting. The weight of the as-received ingot (Ingot 1) is 8 kg. An ingot with a small amount of alloying elements (Ingot 2) was also fabricated to investigate the effect of alloying elements on etch pits. The chemical compositions of these ingots are listed in Table 1.

The two ingots were forged into square rods with cross-sectional dimensions of 40 mm × 40 mm at temperatures ranging from 1000 to 1150°C. The rods were cut into 3 individual segments, homogenized at 840°C for 2 h, water quenched, stress relieved at 315°C for 4 h, furnace cooled, stabilized at 98°C for 48 h, and furnace cooled a second time. Subsequently, the Invar rods were cut into pieces of specific sizes by wire electrical discharge machining and machined into specimens with dimensions of 15 mm × 10 mm × 5 mm.

Table 1. Chemical composition of the Invar ingots wt%

Sample	Ni	Mn	Al	Ti	Fe
Ingot 1	35.8	0.40	—	—	Balance
Ingot 2	36.1	0.45	0.014	0.064	Balance

The specimens were prepared by a hot mounting press (Simplimet 3000, Buehler, An ITW Company, Illinois, USA), and ground and polished for subsequent observation. An etchant composed of 4 g copper sulfate, 20 mL hydrochloric acid and 20 mL deionized water was utilized with an etch time of 2 min. After etching, an optical microscope (Axiovert, 200, MAT, Zeiss, Oberkochen, Germany), scanning electron microscopes (SSX–550, Shimadzu, Kyoto, Japan, and S–3400N, Hitachi, Tokyo, Japan) and an X-ray diffractometer (D/Max-2500PC, Rigaku, Tokyo, Japan) were employed for the characterization of etch pits in the etched surfaces of Invar specimens.

3. Results and discussion

3.1. Identification of etch pits in the pure Invar specimens

(1) Optical microscope characterization. Fig. 1 shows that the Invar specimen exhibits an austenite grain structure with many twins after etching. The mean grain size of the polycrystalline specimen is approximately 80 μm. Numerous small dark dots are distributed on the etched surface. The identification of these dots is challenging. Because the resolution of the optical microscope is limited, it is difficult to distinguish these dots when they are closely spaced. Additional investigation is required to determine whether these dots comprise second phases.

Fig. 1. Optical microscopy photograph of the pure Invar specimen.

(2) X-ray diffraction (XRD) characterization. An X-ray diffractometer was employed to identify the small dots. As shown in Fig. 2, the X-ray diffraction pattern corresponds with the PDF card No. 47–1405. No obvious diffraction peaks of any second phase could be identified. Thus, the findings indicate the presence of pure $Fe_{0.64}Ni_{0.36}$ in the pure Invar alloy. Considering the single phase in this alloy and the imaging mechanism of the optical microscope, these dark dots were presumed to be small pits.

(3) SEM characterization. SEM was employed to vividly characterize the surface morphology of the sample. The unknown substances that appeared as small dark dots in the optical microphotograph are determined to be etch pits as shown in Fig. 3. The majority of the etch pits have sizes of several micrometers. Etch pits of various shapes, such as

triangle, quadrilateral, and hexagonal, are observed. Note that small pits in an individual grain exhibit the same shape and orientation, whereas the shapes of the etch pits change with grain orientation.

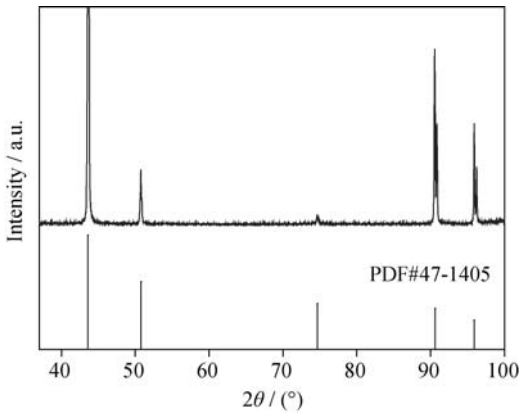

Fig. 2. XRD pattern of the pure Invar specimen.

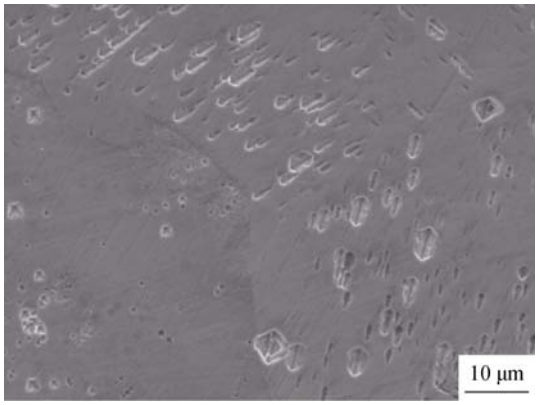

Fig. 3. SEM photograph of typical etch pits in the pure Invar specimen.

3.2. Observation of etch pits in the pure Invar alloy

Etch pit formation is most likely attributed to the preferential nucleation of unit pits at a dislocation, which have a depth of one molecule, and the movement of monomolecular steps across the surface. The relative rates of these two processes affect both the widths and the depths of the etch pits.

When the alloy is properly etched, the dissolution of atoms located on the dislocations is preferred due to the abnormal arrangement of atoms. The etch rates for the crystallographic planes with different atom arrangements vary. Etch pits with specific shapes form on the etched surface of the pure Invar sample.

Although it has not been confirmed that every dislocation that intersects with the etched surfaces of the Invar sample has a corresponding dislocation etch pit under actual circumstances, etch pits are closely related to dislocations in the alloy. The dislocation densities of different grains can be compared by evaluating etch pit densities, and the dislocation behavior can be indirectly evaluated by observation of the etch pits. Using this method, typical dislocation behavior was observed.

(1) Dislocation etch pits arranged on grain boundaries. Etch pits located at grain boundaries are shown in Fig. 4. Because no inclusions or second phases are observed in these etch pits and the shapes of these etch pits are regular, these etch pits can be considered to be dislocation etch pits.

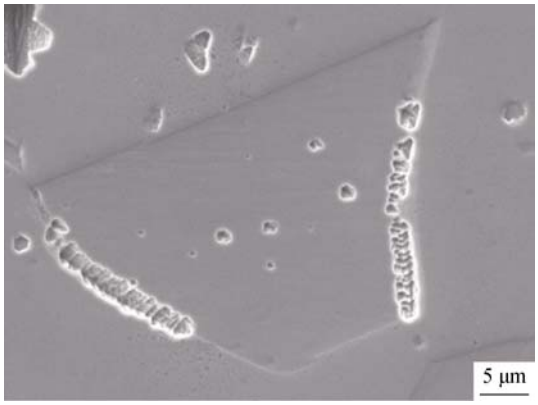

Fig. 4. SEM photograph of etch pits arranged on grain boundaries.

Under certain external forces, dislocations in grains can slip. When the moving dislocations encounter grain boundaries, it is unable for them to pass without sufficient energy. Thus, the dislocations halt at the grain boundaries and arrange along these boundaries. After the Invar sample is etched, rows of dislocation etch pits appear along the grain boundaries.

Although two sides of the shown grain are occupied by dislocation etch pits, only dislocations marked by etch pits on the right side were previously located in this grain because the ends of the dislocation etch pits are positioned here. Dislocations marked by etch pits on the left side migrated from another grain.

(2) Dislocation etch pits gathered on grain tips. Dislocation etch pits were observed on some grain tips, as shown in Fig. 5. Two types of dislocation etch pits are distributed on opposite sides of the grain boundary: etch pits with a triangular shape and etch pits with a quadrilateral shape. This finding reveals a local stress concentration at these grain tips, which may be attributed to the interaction of the two grains caused by thermal expansion and/or deformation.

The quadrilateral-shaped dislocation etch pits are determined to be denser than the triangular-shaped dislocation etch pits. The accumulation of dislocations in a grain may cause dislocation movement in a neighboring grain. Thus,

dislocations marked by triangular-shaped etch pits may be caused by dislocations marked by quadrilateral-shaped etch pits.

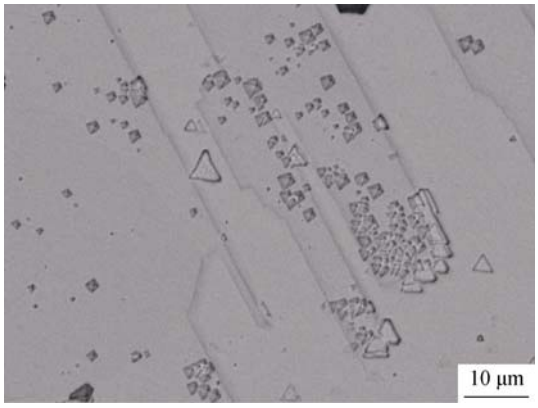

Fig. 5. SEM photograph of etch pits gathered on grain tips.

Microscopically, dislocation movements both within individual grains and across grain boundaries between neighboring grains may cause low-temperature deformation.

(3) Strip-like etch pit clusters passing through multiple grains. Strip-like etch pit clusters were also observed. In a single strip, etch pits with various shapes accumulate in different orientated grains, as shown in Fig. 6. The etch pit clusters may also be attributed to the stress concentration in these strip-like zones. The forging process and the quenching process may produce local stress concentration and dislocation etch pit clusters.

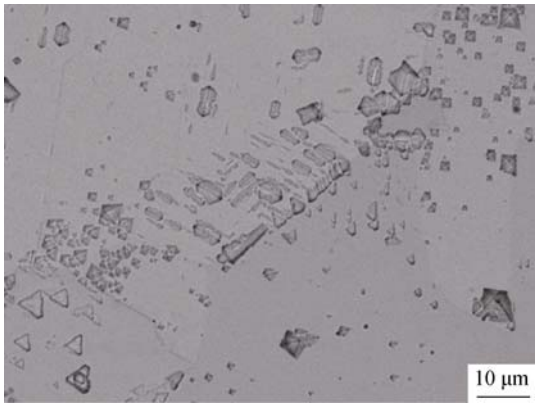

Fig. 6. Strip-like etch pit clusters passing through multiple grains.

3.3. Observation of etch pits in the Invar alloy with the addition of alloying elements

The addition of a small amount of alloying elements including 0.014wt% Al and 0.064wt% Ti to the Invar alloy hindered the detection of dislocation etch pits. The etched surfaces of the Invar samples with alloying elements are coarse and obscure, as shown in Fig. 7.

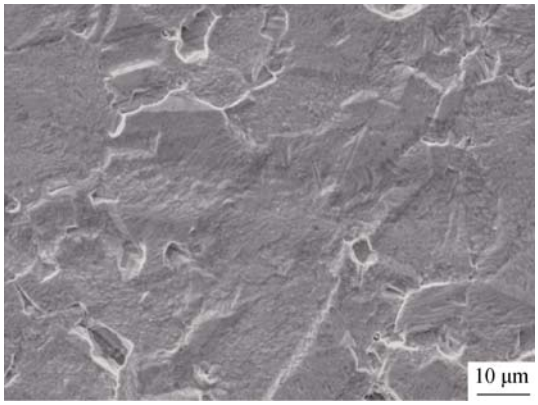

Fig. 7. SEM photograph of an Invar sample with a small amount of alloying elements.

The alloying elements can react with other elements, such as O, C, and N; thus, inclusions and/or second phases including Al_2O_3 and TiC may emerge in the Invar alloy. The motion of dislocations may be impeded by these inclusions and second phases, and dislocation multiplication may occur. Inclusions, second phases and dislocations are abnormal sites with an irregular arrangement of atoms. The dissolution of atoms at these abnormal sites is preferred. Due to a larger number of abnormal sites in the alloy, the number of etch pits increased dramatically, as shown in Fig. 8.

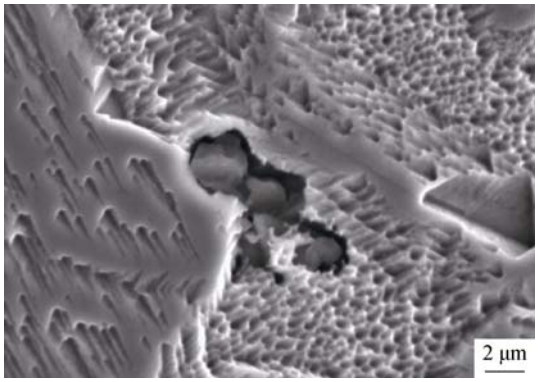

Fig. 8. SEM photograph of inclusions and etch pits after adding a small amount of alloying elements to the Invar alloy.

Few dislocations are located in a specific grain from the pure Invar specimen; thus, a small number of etch pits is detected. These etch pits can freely develop and become larger and deeper. A larger number of etch pits are detected in similarly sized grains from the Invar specimen with alloying elements. Extremely dense etch pits compete with each other and are confined by neighboring grains as they develop. Although the etch pits are considerably denser, their growth is limited compared with etch pits in the pure Invar alloy.

4. Conclusion

Although dislocations can be precisely investigated by means of modern instruments, it remains a suitable method to study the dislocation behavior by observing dislocation etch pits. The advantages of this method include convenient sample preparation and a larger field of view.

Etch pits in two Invar ingots (a pure Invar ingot and an Invar ingot with a small amount of alloying elements) were investigated. Etch pits of various shapes were distinctly observed on the surfaces of the pure Invar specimens using SEM. Etch pits in an individual grain exhibit a specific shape, whereas the shapes of etch pits vary with grain orientation. It was observed that dislocation etch pits arranged along grain boundaries, gathered on grain tips and gathered into strip-like clusters. Local etch pit aggregation is attributed to the local stress concentration caused by thermal expansion and/or deformation. Regarding the close relationship between etch pits and dislocations, the etch pit method can be used to investigate dislocation behaviors in Fe–36wt%Ni Invar alloy.

The addition of a small amount of alloying elements resulted in smaller and less distinct dislocation etch pits in the Invar specimens. Alloying elements react with other elements and subsequently form numerous inclusions and second phases, which produces dislocation multiplication. Etching at extremely dense abnormal sites, such as inclusions, second phases and dislocations, is preferred; as a result, a greater number of dislocation etch pits are detected. The competition among extremely dense etch pits generates smaller etch pits, which complicates the identification of etch pits.

References

[1] J.L. Weyher, P.D. Brown, J.L. Rouvière, T. Wosinski, A.R.A. Zauner, and I. Grzegory, Recent advances in defect-selective etching of GaN, *J. Cryst. Growth*, 210(2000), No. 1-3, p. 151.

[2] S. Mukerji and T. Kar, Etch pit study of different crystallographic faces of L-arginine hydrobromide monohydrate (LAHBr) in some organic acids, *J. Cryst. Growth*, 204(1999), No. 3, p. 341.

[3] F.E.H. Tay, C. Iliescu, J. Jing, and J.M. Miao, Defect-free wet etching through pyrex glass using Cr/Au mask, *Microsyst. Technol.*, 12(2006), No. 10-11, p. 935.

[4] J. Lee, J. Kim, J. Kim, J. Lee, H. Chung, and Y. Tak, Effects of pretreatment on the aluminum etch pit formation, *Corros. Sci.*, 51(2009), No. 7, p. 1501.

[5] D.W. Britt and V. Hlady, *In-situ* atomic force microscope imaging of calcite etch pit morphology changes in undersaturated and 1-hydroxyethylidene-1, 1-diphosphonic acid poisoned solutions, *Langmuir*, 13(1997), No. 7, p. 1873.

[6] S.W. Lee, D.C. Oh, H. Goto, J.S. Ha, H.J. Lee, T. Hanada, M.W. Cho, T. Yao, S.K. Hong, H.Y. Lee, S.R. Cho, J.W. Choi, J. Choi, J.H. Jang, J.E. Shin, and J.S. Lee, Origin of forward leakage current in GaN-based light-emitting devices, *Appl. Phys. Lett.*, 89(2006), No. 13, art. No. 132117.

[7] D. Muto, T. Araki, H. Naoi, F. Matsuda, and Y. Nanishi, Polarity determination of InN by wet etching, *Phys. Status Solidi A*, 202(2005), No. 5, p. 773.

[8] J. Chen, J.F. Wang, H. Wang, J.J. Zhu, S.M. Zhang, D.G. Zhao, D.S. Jiang, H. Yang, U. Jahn, and K.H. Ploog, Measurement of threading dislocation densities in GaN by wet chemical etching, *Semicond. Sci. Technol.*, 21(2006), No. 9, p. 1229.

[9] D.S. Wuu, H.W. Wu, S.T. Chen, T.Y. Tsai, X.H. Zheng, and R.H. Horng, Defect reduction of laterally regrown GaN on GaN/patterned sapphire substrates, *J. Cryst. Growth*, 311(2009), No. 10, p. 3063.

[10] R.T. Bondokov, S.G. Mueller, K.E. Morgan, G.A. Slack, S. Schujman, M.C. Wood, J.A. Smart, and L.J. Schowalter, Large-area AlN substrates for electronic applications: an industrial perspective, *J. Cryst. Growth*, 310(2008), No. 17, p. 4020.

[11] P. Visconti, K.M. Jones, M.A. Reshchikov, R. Cingolani, H. Morkoc, and R.J. Molnar, Dislocation density in GaN determined by photoelectrochemical and hot-wet etching, *Appl. Phys. Lett.*, 77(2000), No. 22, p. 3532.

[12] Z.H. Zhang, Y. Gao, and T. Sudarshan, Delineating structural defects in highly doped n-type 4H-SiC substrates using a combination of thermal diffusion and molten KOH etching, *Electrochem. Solid State Lett.*, 7(2004), No. 11, p. G264.

[13] T. Hino, S. Tomiya, T. Miyajima, K. Yanashima, S. Hashimoto, and M. Ikeda, Characterization of threading dislocations in GaN epitaxial layers, *Appl. Phys. Lett.*, 76(2000), No. 23, p. 3421.

[14] L. Lu, Z.Y. Gao, B. Shen, F.J. Xu, S. Huang, Z.L. Miao, Y. Hao, Z.J. Yang, G.Y. Zhang, X.P. Zhang, J. Xu, and D.P. Yu, Microstructure and origin of dislocation etch pits in GaN epilayers grown by metal organic chemical vapor deposition, *J. Appl. Phys.*, 104(2008), No. 12, art. No. 123525.

[15] J. Pešička, R. Kužel, A. Dronhofer, and G. Eggeler, The evolution of dislocation density during heat treatment and creep of tempered martensite ferritic steels, *Acta Mater.*, 51(2003), No. 16, p. 4847.

[16] Y.C. Shen, G.O. Mueller, S. Watanabe, N.F. Gardner, A. Munkholm, and M.R. Krames, Auger recombination in InGaN measured by photoluminescence, *Appl. Phys. Lett.*, 91(2007), No. 14, art. No. 141101.

[17] F. Kawamura, M. Tanpo, N. Miyoshi, M. Imade, M. Yoshimura, Y. Mori, Y. Kitaoka, and T. Sasaki, Growth of GaN single crystals with extremely low dislocation density by two-step dislocation reduction, *J. Cryst. Growth*, 311(2009), No. 10, p. 3019.

[18] T. Hashimoto, F. Wu, J.S. Speck, and S. Nakamura, A GaN bulk crystal with improved structural quality grown by the ammonothermal method, *Nat. Mater.*, 6(2007), No. 8, p. 568.